Self-Assembled Mesomorphic Complexes of Branched Poly(ethylenimine) and Dodecylbenzenesulfonic Acid

Hsin-Lung Chen* and Ming-Siao Hsiao

Department of Chemical Engineering, National Tsing Hua University, Hsin-Chu, Taiwan 30043, R.O.C

Received September 8, 1998; Revised Manuscript Received January 25, 1999

ABSTRACT: Solid-state complexes of flexible polymers with surfactants (surf) exhibit mesomorphic phase and microphase-separated lamellar morphology. Because the surf molecules are strongly associated with the polymer backbone, the ordered packing of the alkyl tails should be cooperative with the chain packing in the polymer layers which is influenced by chain topology. In this study, the supramolecular structure and thermal properties of the complexes of a highly branched poly(ethylenimine) (PEI) with dodecylbenzenesulfonic acid (DBSA) were investigated. Polarized optical microscopy and small-angle X-ray scattering (SAXS) revealed the presences of mesomorphic phases and microphase-separated lamellar morphology in the complexes. The ordered supramolecular structure was observed not only for the stoichiometric composition but over a wide composition range. The thicknesses of polymer and surf layers were determined from the one-dimensional correlation function. The surf layer thickness varied with complex composition. The glass transition temperature of polymer layers was raised by complexation because of the stiffening of polymer chains. Complexation with DBSA also enhanced the thermal stability of PEI, where the thermal decomposition temperature can be raised by as much as 50 °C.

Introduction

Complexes of flexible polymers with amphiphilic surfactants (surf) form a novel class of materials that exhibit interesting combinations of phase structure and properties. The driving forces of complexation are the attractive interaction between the polymer and the polar head of surf and the hydrophobic interaction of the alkyl tails in solution.[1] Polymer(surf) complexes in aqueous solutions have been investigated in detail (e.g., refs 2−6). On the other hand, the complexes in the bulk state have just attracted attention recently.[7−29] In the bulk, polymer(surf) complexes self-organize into structural patterns of various length scales through the delicate balance of attractive and repulsive interactions. The important characteristics of the complexes include the following:

(1) Comblike molecular configuration, where surf molecules are strongly associated with the polymer backbone giving rise to a comb polymer formed via noncovalent interactions.[1] The alkyl tails of the surf and the polymer chains are highly stretched due to the excluded-volume effect of the alkyl tails.

(2) Microphase-separated nanostructure, where the complexes self-organize to form a nonpolar surf phase and a polar polymer phase when the polar−nonpolar repulsion between the polymer backbone and the alkyl tails is sufficiently strong.[8] Similar to block copolymers, the morphological pattern is governed by the volume fraction and the length of alkyl tails. Lamellar morphology consisting of alternating polymer and surf layers was predominantly observed. Antonietti et al. suggested the undulating lamellar structure where increasing alkyl length induces a spontaneous interfacial curvature toward the other phase that destabilizes the lamellar morphology and eventually leads to the new phase structures.[7,8] The lamellar morphology in the complexes was typically revealed by small-angle X-ray scattering (SAXS). Direct imaging of the lamellar structure in the poly(4-vinylpyridine) (PVP)−4-nonadecylphenol complex has recently been accomplished by Ikkala and ten Brinke et al. using transmission electron microscopy (TEM).[25]

(3) Mesomorphic phases, where high degrees of stretching of the nonmesogenic alkyl tails and polymer chains impart liquid crystalline order to the complex.[7,10] The birefringent pattern typical of liquid crystals may be identified under polarized optical microscopy (POM).

Most literature works concerning polymer(surf) complexes have dealt with the solid-state complexes of polyelectrolytes with oppositely charged surfs; in other words, complexation was achieved through electrostatic interactions. Antonietti et al. investigated the complexes of poly(styrenesulfonate) with alkyltrimethylammonium.[7] Tirrell and MacKnight et al. studied the coupling between complexation and the ordered conformation of polypeptides in the complexes of synthetic polypeptides with oppositely charged surfs.[19−20,24] Ikkala and ten Brinke et al. investigated the complexes of PVP with dodecylbenzenesulfonic acid (DBSA).[10] Although PVP is not a polyelectrolyte itself, proton transfer from DBSA to PVP rendered electrostatic interaction in the complexation. In addition to electrostatic interactions, complexation through other types of polymer−surf interaction has been realized recently. Ikkala and ten Brinke et al. discovered the complexation between PVP and alkylphenols through hydrogen bonding.[15,17,22,25] They also demonstrated the complex formation through transition metal coordination between Zn cations in zinc dodecylbenzenesulfonate and the pyridine amines in PVP.[11]

Since both attractive and repulsive interactions are involved and the polymer chains are highly stretched in polymer(surf) complexes, the balances between the interaction energies and the loss in chain conformational entropy should closely control the phase structure of the complexes. Therefore, the morphological structure

* To whom correspondence should be addressed.

10.1021/ma981417g CCC: $18.00
Published on Web 04/08/1999

should depend on the parameters that may influence the energetic and entropic balances. These include the types of polymer−surf interactions, length of alkyl tail, volume fraction of surf, and temperature. Another possible factor is the topology of polymer chain. Because surf molecules are tightly associated with the polymer backbone, the ordered packing of alkyl tails in the surf layer should be cooperative with the chain packing in the polymer layers which is influenced by chain topology. The ordered packing of branched polymer chains is obviously more restricted than linear chains. So one question is whether it is possible to obtain ordered supramolecular structure in the complexes with branched polymers as in the linear polymer complexes. Ujiie et al. recently studied the complexes of a branched low molecular weight poly(ethylenimine) (PEI) with *n*-alkanoic acids.[29] This study focused on the stoichiometric complexes of branched PEI with the alkanoic acids of various alkyl chain lengths. Lamellar mesophases were observed in the complexes, indicating that ordered supramolecular structure can be formed in the stoichiometric complexes of this branched polymer.

In the present study, the feasibility of obtaining ordered supramolecular structure in branched polymer(surf) complexes is further demonstrated by considering the complexes of branched PEI with another acid type surf, dodecylbenzenesulfonic acid (DBSA). The ordered structure reported here is not restricted to the stoichiometric composition but covers a wide composition range. PEI is a water-soluble polymer. The commercial grades of PEI are highly branched which adopts the bushlike structure.[30] The aliphatic amine groups in PEI are more basic than the pyridine amine in PVP, and they are thus more prone to be protonated by DBSA. Complexation between PEI and DBSA may proceed via proton transfer from DBSA to the amine groups in PEI, giving rise to the complexes with electrostatic interaction. In this study, SAXS and POM are utilized to probe the morphological structure including mesomorphic phase and microphase-separated morphology of PEI(DBSA) complexes. The complex structure and the thermal properties will be discussed as a function of composition.

Experimental Section

Materials and Sample Preparation. Poly(ethylenimine) (M_w = 25 000) was acquired from Aldrich. The surfactant DBSA was obtained from Tokio Kasei, Japan. The structure according to the manufacturer is the following:

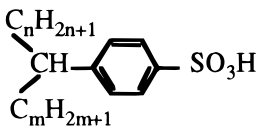

where the dominant length of the alkyl chain ($n + m + 1$) is 12. Such a chemical structure represents a surfactant with double alkyl tails. PEI(DBSA) complexes were prepared by mixing the desired amount of PEI and DBSA in water at room temperature. The concentration of PEI and DBSA in the aqueous solution was 0.5 wt %. The resulting precipitates were isolated by filtration, washed with water, and dried in vacuo at 60 °C for 3 days.

Polarized Optical Microscopy. The mesomorphic structure of PEI(DBSA) complexes was observed by a Pac Hund polarized optical microscope equipped with a Linkam HFS 91 hot stage. The samples were prepared as thin films between two glass slides.

SAXS Measurements. SAXS measurements were performed with the sample temperature controlled at room temperature (ca. 27 °C) and 75 °C. The power of X-ray source was operated at 200 mA and 40 kV. The X-ray source is a 18 kW rotating anode X-ray generator (Rigaku) equipped with a rotating anode Cu target. The incident X-ray beam was monochromated by a pyrolytic graphite, and a set of three pinhole inherent collimators were used so that the smearing effects inherent in slit-collimated small-angle X-ray cameras can be avoided. The sizes of the first and second pinhole are 1.5 and 1.0 mm, respectively, and the size of the guard pinhole before the sample is 2.0 mm. The scattered intensity was detected by a two-dimensional position sensitive detector (ORDELA model 2201X, Oak Ridge Detector Laboratory Inc.) with 256 × 256 channels (active area 20 × 20 cm^2 with ∼1 mm resolution). The sample-to-detector distance is 2000 mm long. The beam stop is a round lead disk of 18 mm in diameter. All data were corrected by the background (dark current and empty beam scattering) and the sensitivity of each pixel of the area detector. The area scattering pattern has been radially averaged to increase the efficiency of data collection compared with one-dimensional linear detector. Data were acquired and processed on an IBM-compatible personal computer. The intensity profile was output as the plot of the scattering intensity (I) vs the scattering factor, $q = 4\pi/\lambda \sin(\theta/2)$ (θ = scattering angle).

Infrared Spectroscopy. Infrared spectra of PEI(DBSA) complexes were obtained using a Nicolet 320 FTIR spectrometer. Samples were prepared by melt casting directly onto the KBr windows at 80 °C. IR spectra were collected under nitrogen atmosphere with a resolution of 2 cm^{-1} and computer-averaging a total of 32 scans.

Differential Scanning Calorimeter and Thermogravimetric Analysis. Thermal transitions of PEI(DBSA) complexes were measured with a TA Instrument 2000 differential scanning calorimeter (DSC) equipped with the RCS cooling system. The hating scans were performed from −60 to 150 °C at a heating rate of 20 °C/min. Thermal transitions were collected from the second heating scans. Thermogravimetric analysis (TGA) was conducted with a Seiko SII EXSTAR6000 TGA from 50 to 800 °C at 10 °C/min.

Results and Discussion

Complex Composition and Binding Mode. The actual composition of the complexes is denoted by "x" which expresses the average number of DBSA molecules bound with a PEI unit. x is distinguished from the prescribed composition (x') given by the feed ratio of polymer and surf in the complex preparation. The actual composition was determined by the elemental analysis of the nitrogen content in the precipitate. Figure 1a compares the measured nitrogen content with the prescribed value for various complex compositions. The measured contents agree with the calculated values at high prescribed compositions of $x' \geq 0.75$, while deviation from the prescribed composition is observed at a lower degree of complexation. Figure 1b plots the actual composition against the prescribed composition. The actual composition starts to deviate from the prescribed value at intermediate levels of complexation, where x is always higher than x'. The deviation is larger at lower degree of complexation.

Deviation from the prescribed composition may be connected with the binding process of surf molecules in the complex formation. The binding of surf molecules in aqueous solution is highly cooperative, where the binding process neighboring a "docked surf" is much faster than the primary binding.[4,6,31−33] Such a binding process is sometimes called the "zipper mechanism". The zipper binding may give rise to 1:1 stoichiometry for the complex, and the self-assembly of the stoichiometric complex results in precipitation. The polymer chains without or with low degree of complexation remain in

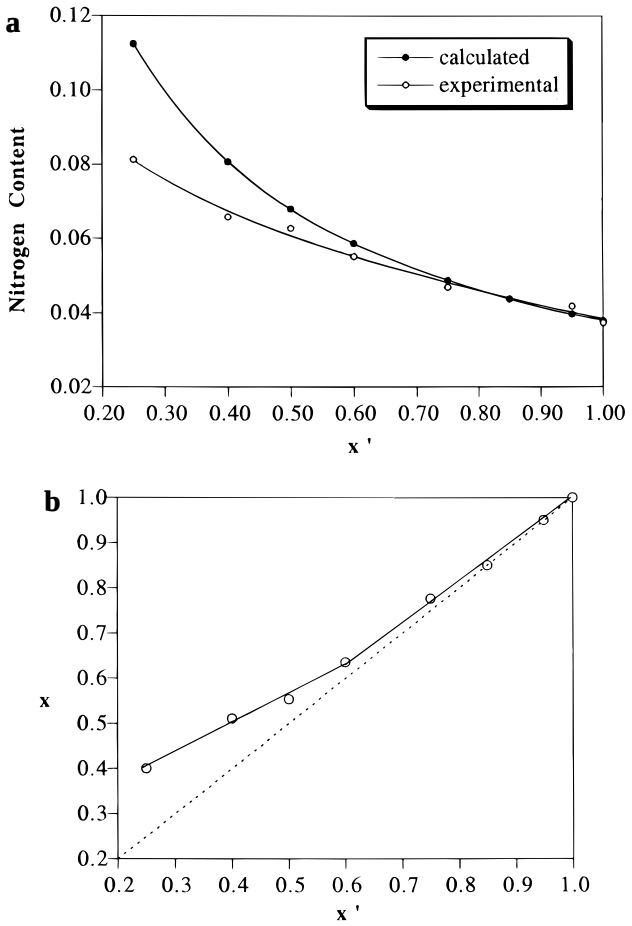

Figure 1. (a) Comparison between the nitrogen contents determined from elemental analysis (open circle) and that calculated from the prescribed composition (filled circle). (b) Plot of the actual composition (x) vs the prescribed composition (x') for PEI(DBSA) complexes.

solution. Judging from the measured complex composition, the complexation of PEI and DBSA does not follow the 1:1 stoichiometry. This may be due to the branching nature of PEI which contains primary, secondary, and tertiary amines. The relative basicity and hence the tendency of the amine groups to be protonated follows the order of 1° > 2° > 3°.[30] Once these three types of amine groups are distributed statistically in the PEI backbone, the zipper binding may not be as effective as in a linear PEI because the amine groups of uneven reactivity are distributed in the chain.

The binding mode of PEI(DBSA) complexes was investigated by FTIR. Figure 2 presents the FTIR spectra in the region of 800−1300 cm^{-1}. Pure DBSA shows a band at 900 cm^{-1} which corresponds to the SO_3H absorption.[10] This band almost completely vanishes upon complexation with PEI and is replaced by a band due to SO_3^- at ca. 1230 cm^{-1}. These spectral perturbations demonstrate complete proton transfer from DBSA to PEI and are in parallel with the observations for PVP(DBSA) complexes.[10]

Microphase-Separated Morphology and Mesomorphic Phase. The microphase-separated morphology of PEI(DBSA) complexes was probed by SAXS. Figure 3 displays the SAXS profiles of the complexes at room temperature. A scattering peak corresponding to the long period of ca. 2.8 nm is observed over the composition range investigated. The SAXS peak may indicate the formation of lamellar morphology in the

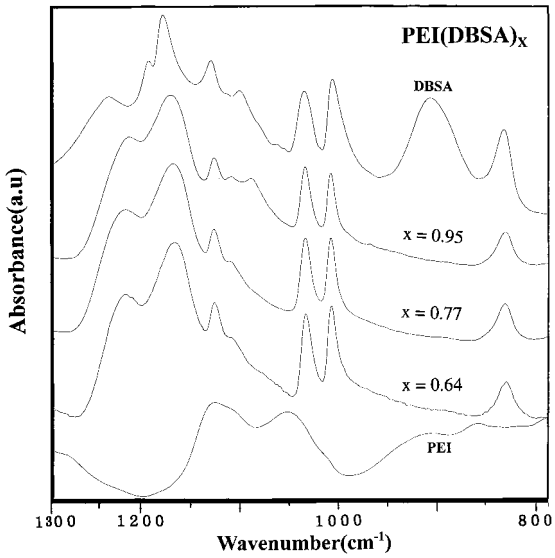

Figure 2. FTIR spectra in the region of 800−1300 cm^{-1} for PEI(DBSA) complexes. The composition is indicated in the figure.

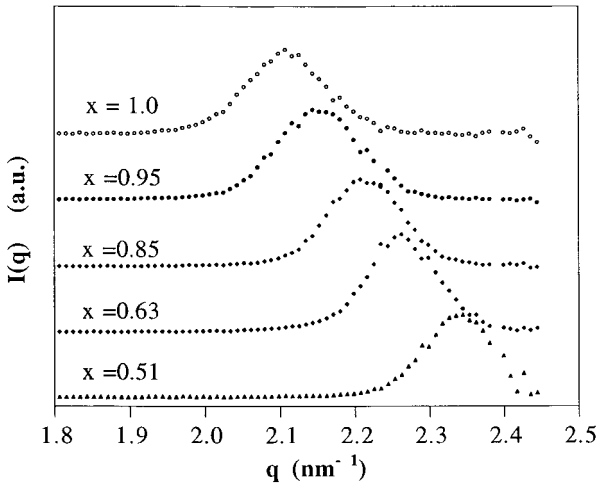

Figure 3. Room-temperature SAXS profiles of PEI(DBSA) complexes.

complexes. The scattering peak shifts to higher angle with decreasing degree of complexation, implying that the long period (L) calculated from the Bragg's law decreases. The SAXS instrument utilized here was unable to detect the second-order peak due to the limitation in the maximum accessible q. To reveal the second-order peak, wide-angle X-ray diffraction (WAXD) was conducted for the stoichiometric composition. Figure 4 shows the WAXD pattern. A second-order peak with a considerably lower intensity than the first-order diffraction can be identified from the pattern. Since no crystalline diffraction is observed, the alkyl tails in the surf layer were not crystalline. It is noted that not all polymer(surf) complexes exhibiting lamellar morphology show the second-order peak. This may be attributed to the comparable volume fraction of the polymer and surf layers[34] or the correlation in the lamellar stacks being restricted to several adjacent layers of polymers.[35,36]

In the case where the second-order peak is absent, observation of a SAXS peak may not be sufficient to support the formation of lamellar morphology in polymer(surf) complexes.[17] In the disordered state, the complexes may exhibit the characteristic block copolymer-like concentration fluctuation (correlation hole effect),

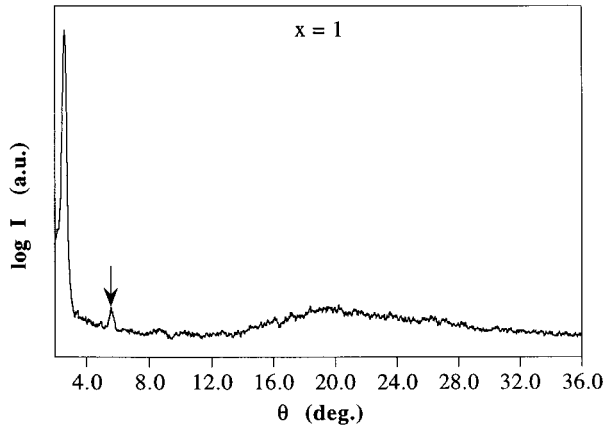

Figure 4. Room-temperature WAXD pattern of stoichiometric PEI(DBSA) complex. The second-order peak is indicated by the arrow.

which can also lead to a SAXS peak.[17,37] The lamellar morphology must be further confirmed with other experimental techniques such as electron microscopy and POM. Observation of birefringent pattern under POM would indicate the formation of mesomorphic phase and along with the SAXS peak should establish the existence of lamellar morphology in the complexes.

Figure 5 displays the polarized optical micrographs of PEI(DBSA) complexes at room temperature (ca. 27 °C). Both PEI and DBSA are amorphous at room temperature, so their POM micrographs are totally dark. On the other hand, birefringent patterns signifying the formation of mesomorphic phases were identified for the complexes. It is noted that the micrographs of $x = 0.40$ were taken after shearing the complexes between two glass slides. Very nice fibrous structure was formed through such a deformation. Isotropization of the mesomorphic phases was not observed until the thermal degradation. The repulsion between the polar polymer layer and the nonpolar surf layer appeared to be sufficiently strong to stabilize the mesomorphic structure prior to thermal degradation.

Combining the observed mesomorphic phase with the SAXS peak, it is established that branched PEI(DBSA) complexes display microphase-separated lamellar morphology. The ordered supramolecular structure is observed not only for the stoichiometric composition but over the composition range investigated ($x = 0.4-1.0$). The high branching level of PEI chains did not undermine the ordered packing of alkyl tails in the complexes, and like linear polymer complexes, branched polymer complexes can also display ordered supramolecular structure over a wide composition range. To allow the alkyl tails bound with a given "polymer sublayer" (a polymer layer is formed by two polymer sublayers) to align along the same direction, the branched chains must not only be highly stretched but also have to lie almost flat, as depicted in Figure 6a. If the chain branches adopted a rather random orientation, as shown in Figure 6b, there would have no long-range correlation in the orientational order of the alkyl tails, and formation of an orderly packed surf layer is impossible. The complexes of linear PEI with DBSA are currently under study with the attempt to reveal the chain topology effect on the ordered structure and the minimum required composition for ordered structural formation.

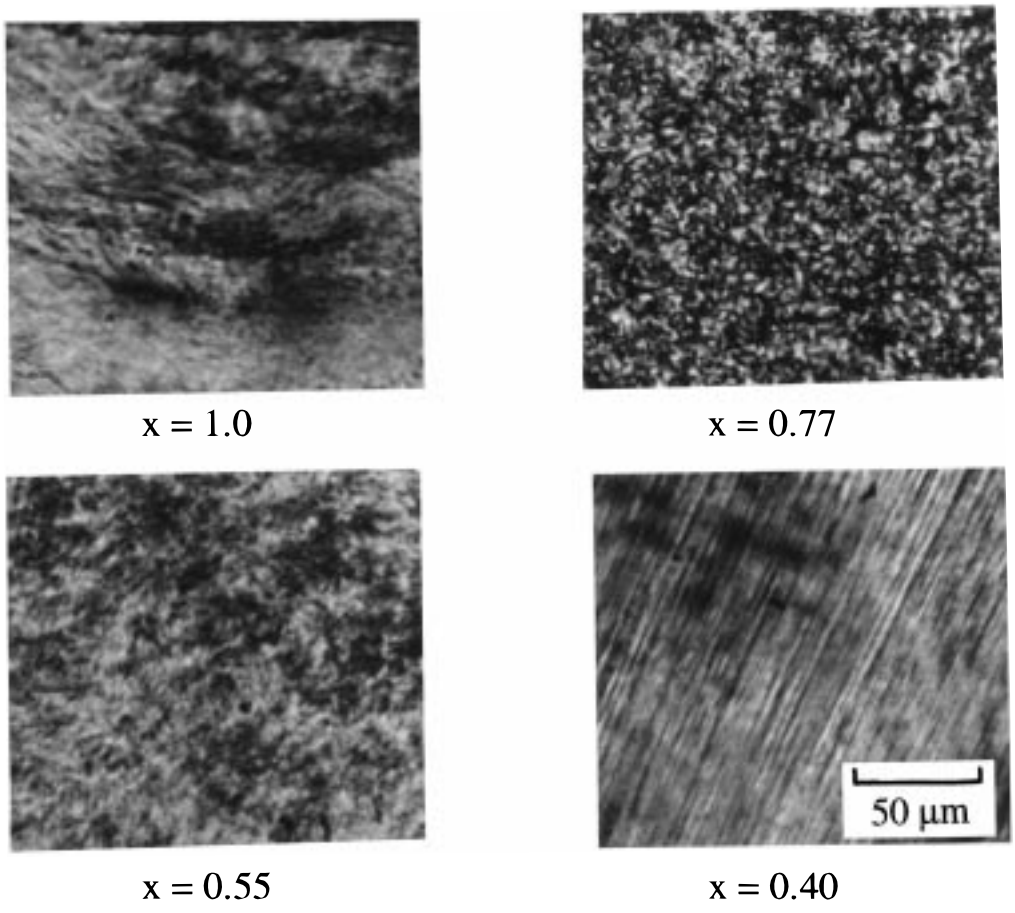

Figure 5. POM micrographs of PEI(DBSA) complexes. The complex compositions are indicated in the figure.

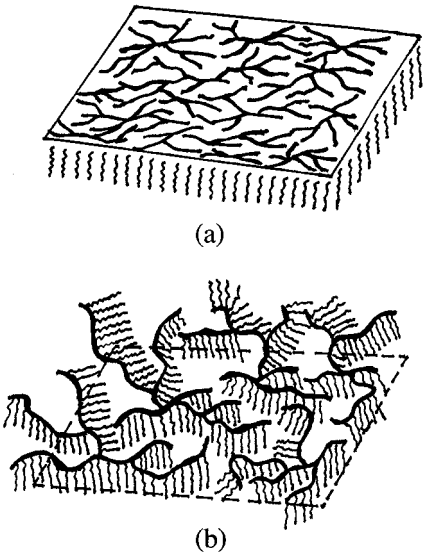

Figure 6. Schematic presentations showing (a) the branched PEI chains lie flatly on the same plane and (b) the chain branches adopt a rather random orientation. The alkyl tails are allowed to direct toward the same direction for (a), and thus an orderly packed surf layer can be formed. Formation of a surf layer is impossible for (b). Only a single alkyl tail is drawn for a DBSA molecule for simplicity.

The lamellar morphology in the complexes consists of alternating polymer and surf layers. Since the lamellar morphology closely resembles the lamellar stack structure in semicrystalline polymers, the one-dimensional correlation function conventionally used to deconvolute the thicknesses of crystal and amorphous layers from the long period was applied to determine the polymer and surf layer thickness.[38] The one-dimensional correlation function is defined as

$$\gamma(z) = \frac{1}{\gamma(0)}\int_0^\infty I(q)q^2 \cos(qz)\, dq \qquad (1)$$

where z is the direction along which the electron density is measured. $\gamma(0)$ is just the scattering invariant:

$$\gamma(0) = Q = \int_0^\infty I(q)q^2\, dq \qquad (2)$$

Since the experimentally accessible q range is finite, extrapolation of intensity to both low and high q is necessary for the integrations. Extrapolation to zero q was accomplished by linear extrapolation, and extension to large q was performed using the Porod−Ruland model.[39−42] The background intensity arising from thermal density fluctuation was subtracted from the overall intensity prior to the correlation function calculation. Figure 7 demonstrates the determination of the layer thickness from the correlation function. The maximum yields the average size of the long period; it generally corresponds to its most probable value, while the long period calculated directly from the scattering peak was considered as weight-average value.[38,43] Intersection of the baseline with the straight line extended from the self-correlation triangle yields the average thickness of the thinner layer in the lamellar stacks.[38] The thinner layer is considered as the polymer layer.

Figure 8a plots the long period determined from the correlation function against complex composition for the two measuring temperatures. At room temperature, the long period remains approximately constant at ca. 2.8 nm for $x \leq 0.85$ and then increases with degree of complexation when x exceeds 0.85. On the other hand, the long period stays at a constant value throughout the composition range at 75 °C. Figure 8b shows the polymer layer thickness (l_p) and surf layer thickness (l_s) as a function of complex composition. At both temperatures, the polymer layer thickness of 1.15 nm remains almost constant with composition, and the thickness is relatively unaffected by temperature for a given composition. At room temperature, the surf layer has the thickness of ca. 1.65 nm for the degrees of complexation

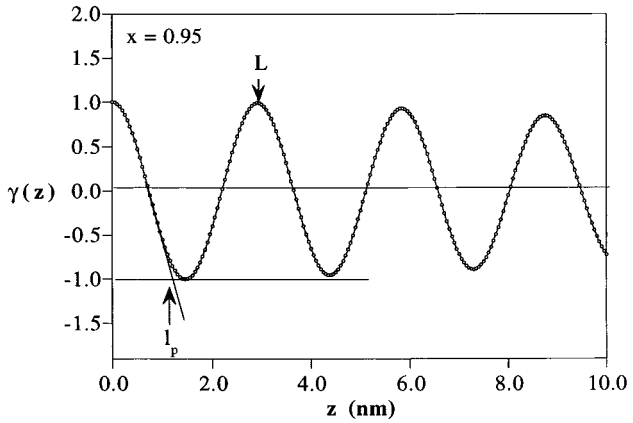

Figure 7. Determinations of the polymer layer thickness (l_p) and long period (L) from the one-dimensional correlation function.

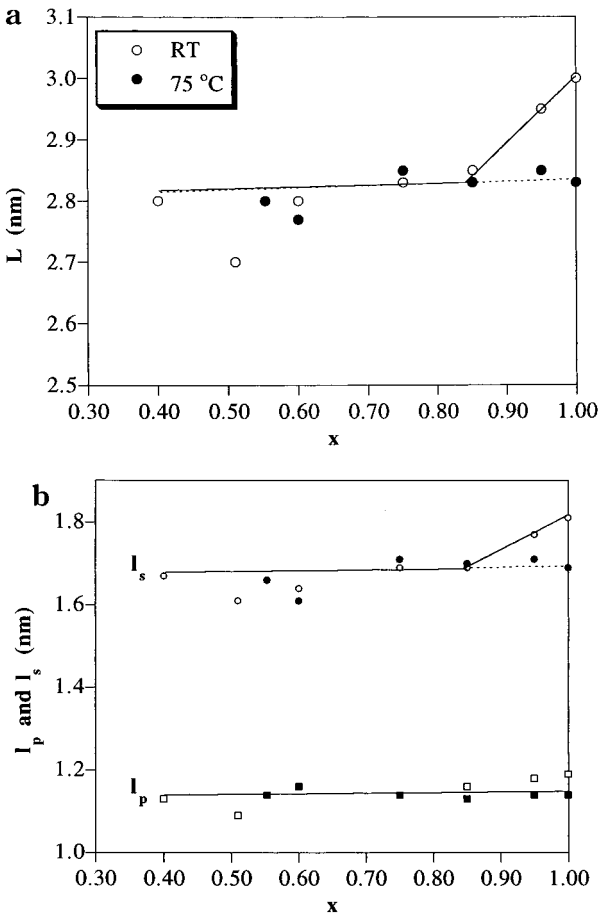

Figure 8. Composition variations of (a) long period (L) and (b) polymer layer thickness (l_p) and surf layer thickness (l_s) of PEI(DBSA) complexes. The open symbols stand for the data obtained at room temperature, while the filled symbols signify the data collected at 75 °C.

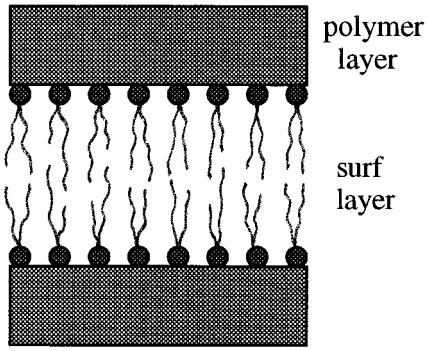

Figure 9. Schematic presentation for the layer structure of PEI(DBSA) complexes.

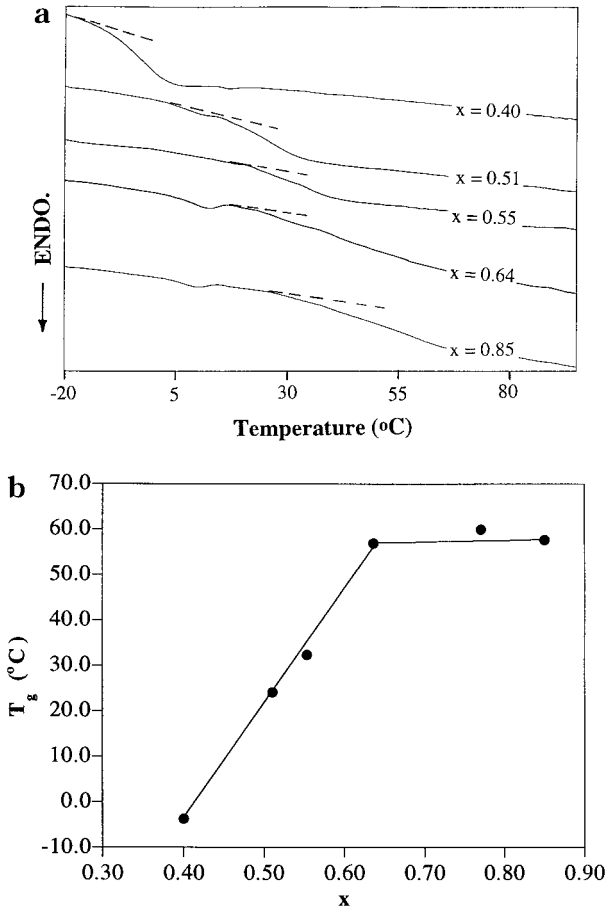

Figure 10. (a) DSC thermograms and (b) composition variation of glass transition temperature of PEI(DBSA) complexes. The peaks at ca. 5 °C are the noises of the DSC instrument.

of $x \leq 0.85$ and increases when x exceeds 0.85 to 1.81 nm for full complexation. The surf layer thickness is relatively independent of composition at 75 °C. For $x >$ 0.85, the surf layer is thinner at 75 °C than that at room temperature. This means the alkyl chains became less stretched as the complexes with high degree of complexation were heated to 75 °C. Increasing temperature may exert two effects on the thickness of the surf layer. The thermal expansion effect tends to increase the thickness as temperature rises. On the other hand, raising temperature may increase the population of gauche conformation, which tends to reduce the layer thickness. The surf layer thickness is controlled by the interplay between these two opposing effects. As the temperature was elevated from room temperature to 75 °C, the effect of increasing gauche population dominated

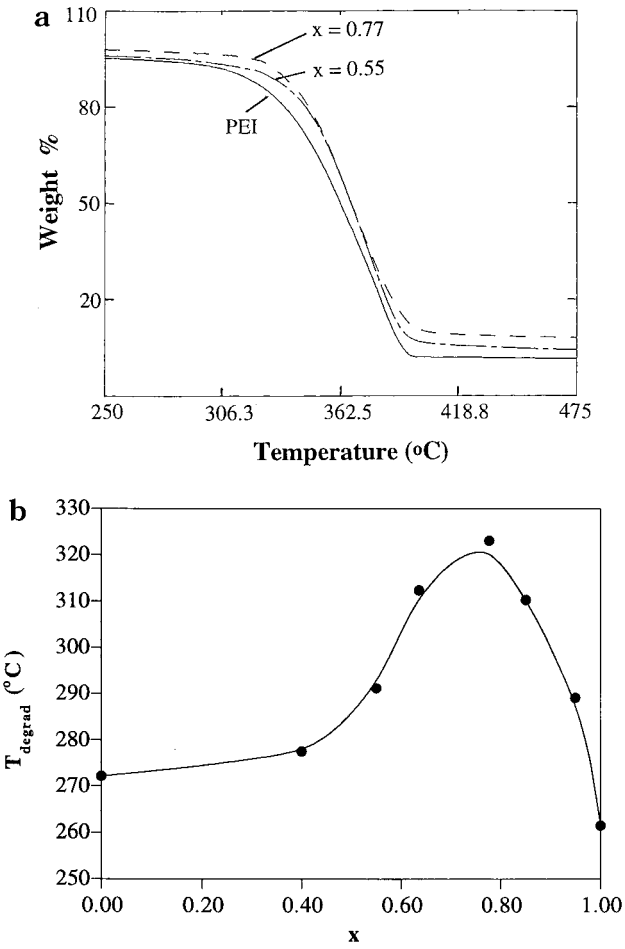

Figure 11. (a) TGA thermograms and (b) composition variation of initial degradation temperature of PEI(DBSA) complexes.

over the thermal expansion effect, leading to the reduction of surf layer thickness.

If each DBSA molecule is assumed to contain only one alkyl chain, the fully extended length of 1.66 nm can be calculated for the nonpolar tail. The actual extended length would be smaller than this value since a DBSA molecule has two alkyl tails. The length of 1.66 nm is smaller than the thickness of the surf layer at high degree of complexation, meaning that a surf layer is not composed of the alkyl tails associated with only one polymer layer. A surf layer may be formed through the tail-to-tail arrangement of the alkyl tails bound with two polymer layers, as illustrated in Figure 9.

Thermal Properties. PEI(DBSA) complexes with low to intermediate degree of complexation are ductile materials at room temperature but turn into brittle materials with high degree of complexation. The mechanical properties of this complex may thus be tuned through composition control. The DSC thermograms of PEI(DBSA) complexes are displayed in Figure 10a. A glass transition temperature was identified up to $x =$ 0.85. The observed T_g is associated with the glass transition of the polymer layers. Figure 10b plots the T_g as a function of complex composition. T_g increases with degree of complexation up to $x = 0.64$ and then levels off at 58 °C. The increase in T_g may be attributed to the stiffening of polymer chains upon complexation.

Since DBSA is strongly associated with PEI through electrostatic interaction, the thermal stability of PEI may also be affected by complexation. Figure 11a shows

the TGA thermograms of the complexes under nitrogen atmosphere. The thermal stability of PEI is enhanced upon complexation. Figure 11b plots the initial degradation temperature against the complex composition. The variation of degradation temperature with x shows a maximum instead of a monotonic increase. The reason for the existence of such a maximum is not known at the current stage. The maximum thermal stability is achieved at $x = 0.77$ where the degradation temperature is raised by as much as 50 °C.

Conclusions

Morphological structure and thermal properties of the solid-state complexes of DBSA with branched PEI have been characterized in this study. Mesomorphic phases and microphase-separated lamellar morphology were observed not only for the stoichiometric composition but over the composition range investigated ($x = 0.4-1.0$). The high branching level of PEI chains did not undermine the ordered packing of alkyl tails in the complexes, and like linear polymer complexes, branched polymer complexes can display ordered supramolecular structure over a wide composition range. The thicknesses of polymer and surf layers determined from the one-dimensional correlation function varied with composition and temperature. The balances between the interaction (repulsive and attractive) energies and the loss in chain conformational entropy were likely to control the phase structure of the complexes. The thermal properties of PEI can be modified by complexation with DBSA. The glass transition of PEI was increased by complexation because of chain stiffening. The thermal stability of PEI was also enhanced, where the degradation temperature can be raised by as much as 50 °C.

Acknowledgment. H.-L. Chen dedicates this paper to the memory of his thesis advisor, Professor Roger S. Porter, who passed away on August 25, 1998. This work is supported by the National Science Council, R. O. C., under Grant NSC 88-2216-E-007-012.

References and Notes

(1) Fredrickson, G. H. *Macromolecules* **1993**, *26*, 2825.
(2) Hayagawa, K.; Santerre, J. P.; Kwak, J. C. T. *J. Phys. Chem.* **1982**, *86*, 3866.
(3) Hayagawa, K.; Santerre, J. P.; Kwak, J. C. T. *J. Phys. Chem.* **1983**, *87*, 506.
(4) Hayagawa, K.; Santerre, J. P.; Kwak, J. C. T. *Macromolecules* **1983**, *16*, 1642.
(5) Goddard, E. D. *Colloids Surf.* **1986**, *19*, 301.
(6) Chandar, P.; Somasundaran, P.; Turro, N. J. *Macromolecules* **1988**, *21*, 950.
(7) Antonietti, M.; Conrad, J.; Thunemann, A. *Macromolecules* **1994**, *27*, 6007.
(8) Antonietti, M.; Burger, C.; Effing, J. *Adv. Mater.* **1995**, *7*, 751.
(9) Antonietti, M.; Kaul, A.; Thunemann, A. *Langmuir* **1995**, *11*, 2633.
(10) Ikkala, O.; Ruokolainen, J.; ten Brinke, G.; Torkkeli, M.; Serimaa, R. *Macromolecules* **1995**, *28*, 7088.
(11) Ruokolainen, J.; Tanner, J.; ten Brinke, G.; Ikkala, O.; Torkkeli, M.; Serimaa, R. *Macromolecules* **1995**, *28*, 7779.
(12) Tal'roze, R. V.; Kuptsov, S. A.; Sycheva, T. I.; Bezborodov, V. S.; Plate′, N. A. *Macromolecules* **1995**, *28*, 8689.
(13) Yang, C. Y.; Smith, P.; Heeger, A. J.; Cao, Y.; Osterholm, J.-E. *Polymer* **1994**, *35*, 1142.
(14) Antonietti, M.; Radloff, D.; Wiesner, U.; Spiess, H. W. *Macromol. Chem. Phys.* **1996**, *197*, 2713.
(15) Ruokolainen, J.; ten Brinke, G.; Ikkala, O.; Torkkeli, M.; Serimaa, R. *Macromolecules* **1996**, *29*, 3409.
(16) Antonietti, M.; Maskos, M. *Macromolecules* **1996**, *29*, 4199.
(17) Roukolainen, J.; Torkkeli, M.; Serimaa, R.; Vahvaselka, S.; Saariaho, M.; ten Brinke, G.; Ikkala, O. *Macromolecules* **1996**, *29*, 6621.
(18) Antonietti, M.; Wenzel, A.; Thunemann, A. *Langmuir* **1996**, *12*, 2111.
(19) Ponomarenko, E. A.; Waddon, A. J.; Bakeev, K. N.; Tirrell, D. A.; Macknight, W. J. *Macromolecules* **1996**, *29*, 4340.
(20) Ponomarenko, E. A.; Tirell, D. A.; MacKnight, W. J. *Macromolecules* **1996**, *29*, 8751.
(21) Ober, C. K.; Wegner, G. *Adv. Mater.* **1997**, *8*, 17.
(22) Ruokolainen, J.; Torkkeli, M.; Serimaa, R.; Komanschek, E.; ten Brinke, G.; Ikkala, O. *Macromolecules* **1997**, *30*, 2002.
(23) Vikki, T.; Ruokolainen, J.; Ikkala, O.; Passiniemi, P.; Isotalo, H.; Torkkeli, M.; Serimaa, R. *Macromolecules* **1997**, *30*, 4064.
(24) Ponomarenko, E. A.; Tirrell, D. A.; MacKnight, W. J. *Macromolecules* **1998**, *31*, 1584.
(25) Ruokolainen, J.; Tanner, J.; Ikkala, O.; ten Brinke, G.; Thomas, E. L. *Macromolecules* **1998**, *31*, 3532.
(26) Kato, T.; Ihata, O.; Ujiie, S.; Tokita, M.; Watanabe, J. *Macromolecules* **1998**, *31*, 3551.
(27) Kawakami, T.; Kato, T. *Macromolecules* **1998**, *31*, 4475.
(28) Ruokolainen, J.; Makinen, R.; Torkkeli, M.; Makela, T.; Serimaa, R.; ten Brinke, G.; Ikkala, O. *Science* **1998**, *280*, 557.
(29) Ujiie, S.; Takagi, S.; Sato, M. *High Perform. Polym.* **1998**, *10*, 139.
(30) Molyneux, P. *Water-Soluble Synthetic Polymers: Properties and Behavior*; CRC Press: Boca Raton, FL, 1983; Vols. 1 and 2.
(31) Philips, B.; Dawydoff, W.; Linow, K. J. *Z. Chem.* **1982**, *22*, 1.
(32) Bakturov, E. A.; Bimendina, L. A. *Adv. Polym. Sci.* **1982**, *41*, 99.
(33) Kabanov, V. A.; Zezin, A. B. *Makromol. Chem. Suppl.* **1984**, *6*, 259.
(34) Handlin, D. L. J.; Thomas, E. L. *Macromolecules* **1983**, *16*, 1514.
(35) Shilov, V. V.; Tsukruk, V. V.; Bliznyuk, V. N.; Lipatov, Y. S. *Polymer* **1982**, *23*, 484.
(36) Shilov, V. V.; Tsukruk, V. V.; Lipatov, Y. S. *J. Polym. Sci., Polym. Phys. Ed.* **1984**, *22*, 41.
(37) Huh, J.; Ikkala, O.; ten Brinke, G. *Macromolecules* **1997**, *30*, 1828.
(38) Strobl, G. R.; Schneider, M. *J. Polym. Sci., Polym. Phys. Ed.* **1980,** *18*, 1343.
(39) Ruland, W. J. *J. Appl. Crystallogr.* **1971**, *4*, 70.
(40) Porod, G. *Kolloid-Z.* **1951**, *124*, 83.
(41) Porod, G. *Kolloid-Z.* **1952**, *125*, 51.
(42) Porod, G. *Kolloid-Z.* **1952,** *125*, 108.
(43) Vonk, C. G. *J. Appl. Crystallgr.* **1978**, *11*, 541.

MA981417G